

# Simultaneous determination of bisphenol A and hydroquinone using a poly(melamine) coated graphene doped carbon paste electrode

Juan Peng<sup>1</sup> · Yun Feng<sup>1</sup> · Xiao-Xia Han<sup>1</sup> · Zuo-Ning Gao<sup>1</sup>

Received: 30 January 2016 / Accepted: 3 May 2016 / Published online: 17 May 2016  
© Springer-Verlag Wien 2016

**Abstract** The authors describe an electrochemical sensor for simultaneous determination of bisphenol A (BPA) and hydroquinone (HQ). It is based on a carbon paste electrode doped with graphene and coated with poly(melamine) (PME/GR-CPE). The modified electrode exhibits excellent conductivity, electrooxidative activity and adsorptive capability. The differential pulse voltammetric peaks for HQ and BPA are separated by around 300 mV. Amperometric responses (at 0.5 V for HQ and 0.8 V for BPA; both vs. SCE) are linear for BPA in the 9.0  $\mu\text{M}$  to 1.0 mM concentration range, and for HQ in the 7.0  $\mu\text{M}$  to 1.0 mM concentration range. The respective detection limits are 10.5 nM and 74.0 nM. The sensor is reproducible, highly stable and sensitive. It was applied to the simultaneous determination of HQ and BPA in spiked tap water and waste water.

**Keywords** Sensor · Cyclic voltammetry · Differential pulse voltammetry · Electropolymerization · Water analysis

## Introduction

Phenol compounds are the essential raw materials and byproducts of numerous chemical industries. Some of these compounds can accumulate in the human body through food chain and cause abnormal sexual development and decrease the

average number of human spermatozoa [1]. Bisphenol A (BPA) is a typical endocrine disruptor, which can mimic the body's own hormones and induce the negative health effects [2, 3]. It is widely used in the production of plastics, food containers and packing materials. The release and migration of BPA into the environment or the food are mainly attributed to the leakage of residual monomers or hydrolysates from polycarbonate plastics and epoxy resins or PVC products, under heat and acidic or basic conditions. Exposure to BPA through food and drinking water is potentially detrimental to human health, even at very low concentrations [4]. BPA has been related to chronic diseases and fertility problems [5]. Based on the results generated from toxicological evaluation of the BPA, the specific migration limit (SML) of BPA (from  $\text{mg}\cdot\text{kg}^{-1}$  to  $\text{sub-mg}\cdot\text{kg}^{-1}$  levels), has been set for plastic materials or food containers and packages in different countries [6, 7]. Hydroquinone (HQ) can cause fatigue, headache, tachycardia, and kidney damage in humans [8]. These two compounds usually coexist in our living environment or foods with high toxicity due to their similar chemical structure and properties. Thus, it is essential to develop a rapid, reliable and sensitive method for the simultaneous determination of HQ and BPA in the food and environment.

Several analytical techniques including high performance liquid chromatography (HPLC) [9], liquid chromatography–mass spectrometry (LC–MS) [10], gas chromatography–mass spectrometry (GC–MS) [11], chemiluminescence [12], and fluorescence [13] had been used for the determination of phenol compounds. However, these methods suffered from some problems such as requiring time-consuming sample pretreatment, expensive equipment and low sensitivity. Electrochemical method has some advantages of fast response speed, simple operation, time saving, high sensitivity and feasibility of miniaturization [14]. However, HQ or BPA exhibits slow electron transfer at bare electrodes, which leads to low sensitivity for their detection [15]. Therefore, various nanomaterials including

**Electronic supplementary material** The online version of this article (doi:10.1007/s00604-016-1865-9) contains supplementary material, which is available to authorized users.

✉ Zuo-Ning Gao  
gaozn@nxu.edu.cn

<sup>1</sup> School of Chemistry and Chemical Engineering, Ningxia University, Yinchuan 750021, People's Republic of China

gold nanodendrites [16], carbon nanotubes [17],  $\text{Bi}_2\text{WO}_6$  nanoplates [18], molybdenum disulfide/polyaniline nanocomposite [19], Pt/graphene-carbon nanotubes nanocomposite [20], carbon naocages/reduced graphene oxide composites [21], layered tungsten sulfide-graphene nanocomposite [22] were used to fabricate BPA or HQ sensors with lower detection limit. Pd nanoparticle@ $\text{TiO}_2$  functionalized SiC was also fabricated to constructed electrochemical sensor for simultaneous determination of hydroquinone and bisphenol A [23].

Graphene (GR) has exhibited wide applications in electrochemical sensors due to its superior properties such as large surface, high electrical conductivity, remarkable electrocatalytic activity [24, 25]. Previous works have also demonstrated the excellent electrocatalytic activity of graphene towards BPA oxidation [26, 27]. Here, graphene was doped in carbon paste electrode to improve the electrode conductivity and electrocatalytic activity. Conducting polymers have attracted intense attention owing to their good stability, reproducibility, more active sites, homogeneity in electrochemical deposition, and strong adherence to electrode surface [28]. The polymer such as polypyrrole [29], polyaniline [30, 31], poly(3,4-ethylenedioxythiophene) (PEDOT) [32], poly(dopamine) [33] and polypropylene [34] have been used for biosensor application. Poly(melamine) (PME) with high stability and abundant nitrogen functional groups has been fabricated and used in electrochemical sensors [35–37]. PME film modified glassy carbon electrode has been fabricated for the sensitive determination of guanine, adenine and epinephrine. [35] PME modified pyrolytic graphite or screen-printed carbon electrode was constructed for sensitive detection of serotonin and gallic acid [36, 37]. PME contains amine groups and a benzene ring so it is supposed to provide binding sites for the adsorption and accumulation of hydroquinone and bisphenol and improve the sensitivity.

In this paper, a sensor based on PME coated on graphene doped carbon paste electrode (PME/GR-CPE) was fabricated for simultaneous determination of BPA and HQ. The fabrication schedule of this sensor was illustrated in Fig. 1. The PME/GR-CPE exhibited superior performance such as high conductivity, electrocatalytic activity and adsorptive capability to BPA and HQ. Differential pulse voltammetry was used to simultaneously quantify HQ and BPA in a wider concentration range with high sensitivity under optimal conditions. The sensor showed good stability and reproducibility. The practical application of the sensor was demonstrated by detection of HQ and BPA in tap water and wastewater samples.

## Experimental

### Reagents

HQ and BPA were from Chemical northern suburb of Beijing (China, <http://11687545.mmjf.com/>) and Suzhou Kai-Fu

Chemical Co., Ltd. (China, <http://www.szkc.com.cn>), respectively. Melamine was purchased from Aladdin Reagent Company (Shanghai, China, [www.aladdin-e.com](http://www.aladdin-e.com)). All chemicals were of analytical grade and used without further purification. All solutions were freshly prepared with double deionized water.

### Apparatus

The prepared composites were characterized by scanning electron microscopy (SEM) (JSM-6700F, JEOL, Japan) and Fourier transform infrared spectroscopy (FTIR) (Lumos, Bruker, UK). Raman spectrum was collected in a Renishaw InVia Raman microscope system with exciting laser wavelength of 514 nm, and the laser output power was 20 mW. Electrochemical experiments were performed with a CHI 660C electrochemical workstation (Chenhua, Shanghai, China) with a conventional three-electrode cell. The working electrode was bare carbon paste electrode or modified carbon paste electrode, reference and counter electrode used were a CHI150 saturated calomel electrode (SCE) and a CHI115 (CH instruments Inc.) platinum wires, respectively. All the measurements were carried out at room temperature.

### Fabrication of carbon paste electrode and graphene doped carbon paste electrode

Graphene was prepared by reduction of GO with references' method [38, 39]. The unmodified CPE was prepared by mixing 1.8 g of graphite powder and 0.60 mL of paraffin oil thoroughly in a mortar to form a homogeneous carbon paste. A portion of the carbon paste was pressed into the end of a poly (tetrafluoroethylene) (PTFE) cylindrical electrode body while a copper wire was inserted through the opposite end to establish an electrical contact. The graphene doped CPE was fabricated using the same procedure except the 0.6 mL of GR ( $0.2 \text{ mg mL}^{-1}$ ) into the carbon paste. Appropriate packing was achieved by pressing the surface against a bond paper until a smooth surface was obtained.

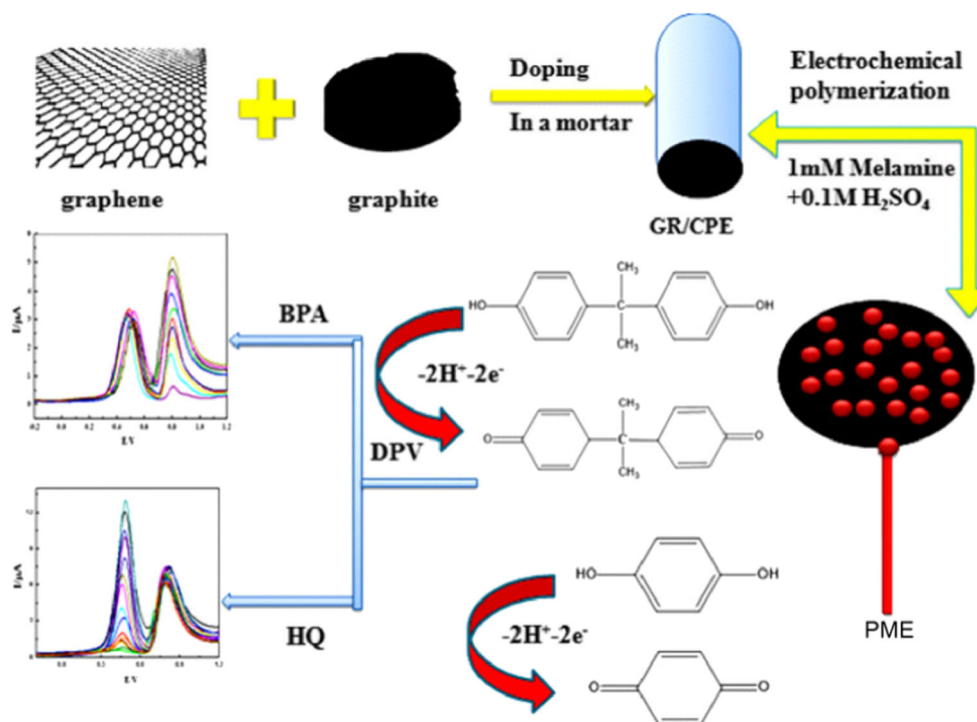
### Electrochemical deposition of poly(melamine) on graphene doped carbon paste electrode

The poly (melamine)/graphene doped CPE was obtained by cyclic voltammetry using graphene doped CPE as working electrode in 0.1 M  $\text{H}_2\text{SO}_4$  containing 1.0 mM melamine in the potential range of  $-0.1$  to  $+1.5$  V at  $100 \text{ mV}\cdot\text{s}^{-1}$  for 10 cycles.

### Electrochemical measurements

The electrochemical impedance spectroscopy was performed in  $5 \times 10^{-3}$  M  $[\text{Fe}(\text{CN})_6]^{3-/4-}$  (1:1) solution containing 0.1 M

**Fig. 1** Illustration scheme of fabrication process of the electrochemical sensor



KCl. The parameters were as follows: frequency range from 1 to  $10^5$  Hz; initiative potential, 0.193 V; amplitude, 0.005 V and quiet time of 2 s. The differential pulse voltammogram was recorded from  $-0.2$  to  $1.2$  V with the parameters of increment potential, 0.004 V; pulse amplitude, 0.05 V; pulse width, 0.0167 s; pulse period, 0.2 s; quiet time, 2 s. The cyclic voltammetry was scanned with scan rate of  $50 \text{ mV}\cdot\text{s}^{-1}$ , sample interval of 0.001 V and quiet time of 10s.

## Results and discussion

### Characterization of the sensor

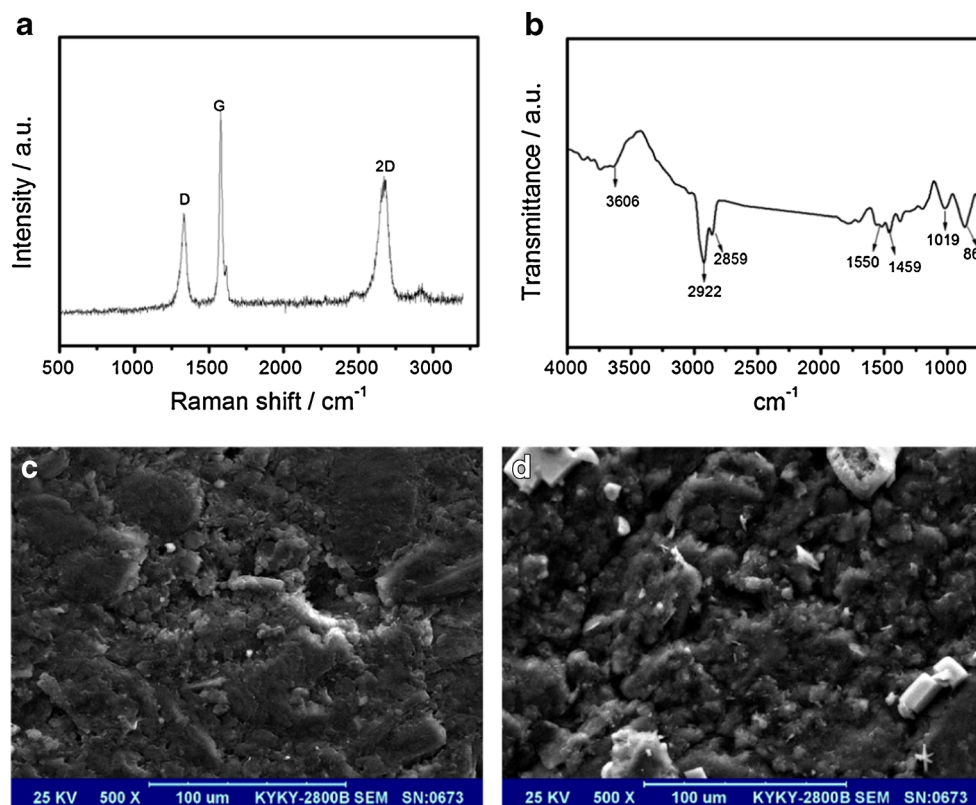
Raman spectroscopy was used to prove the presence of graphene on the electrode. As shown in Fig. 2a, three featured peaks located at  $1369 \text{ cm}^{-1}$  (D-band),  $1590 \text{ cm}^{-1}$  (G-band), and  $2713 \text{ cm}^{-1}$  (2D-band) can be observed for graphene sheets. The D-band corresponds to the  $A_{1g}$  mode breathing vibration of carbon atoms in planar terminations of disordered graphite. The G-band is assigned to  $E_{2g}$  mode of 2D graphite, which is related to vibration of  $\text{sp}^2$ -bonded carbon atoms in the 2D hexagonal lattice [40]. The value of  $I_G/I_D$  is calculated to be 1.9, suggesting the quite high graphitization degree of few-layer graphene. The surface of PME/GR-CPE was also characterized by FTIR (Fig. 2b). This result showed N-H stretching ( $-\text{NH}_2$ ), N-H bending, and C-N stretching bands of the PME at the wave numbers of  $3606 \text{ cm}^{-1}$ ,  $1500\text{--}1600 \text{ cm}^{-1}$ , and

$1019 \text{ cm}^{-1}$ , respectively. This confirmed the formation of PME particles on the GR-CPE.

The surface morphologies of GR-CPE, PME/GR-CPE were characterized by using scanning electron microscopy (SEM). As shown in Fig. 2c, the multiple layers of graphene flakes were observed on the electrode surface. The SEM image (Fig. 2d) of PME/GR-CPE confirmed the presence of PME particles on the electrode surface. The resulting PME/GR-CPE with a three-dimensional structure showed a higher surface area ( $0.0805 \text{ cm}^2$ ) than that of GR-CPE ( $0.0975 \text{ cm}^2$ ), which offered a beneficial interface for electrochemical sensing.

The CVs of potassium ferricyanide on the different electrodes are shown in Fig. 3a. A large peak-to-peak potential separation ( $\Delta E_p$ ) value of 217 mV was observed at the bare CPE, indicating the poor electron-transfer kinetics. The  $\Delta E_p$  value reduced to 175 mV (curve b) and 68 mV (curve c) for GR-CPE and PME/GR-CPE, respectively. Both the cathodic and anodic peak currents significantly enhanced after modifying with graphene due to the good conductivity and electrocatalytic activity of graphene. The cationic, nitrogen-rich PME surface was thought to concentration more anionic ferricyanide than that of the GR-CPE due to the electrostatic attraction. Thus, higher current responses were observed at PME/GR-CPE (Curve c in Fig. 3a). Electrochemical impedance spectrum (EIS) was employed to monitor the impedance changes in the sensor fabrication process. The impedance spectrum includes a semicircle portion and a linear part. The diameter of the semicircle is equivalent the electron-transfer resistance ( $R_{et}$ ), corresponding to the electro-transfer limited

**Fig. 2** **a** Raman spectra of GR-CPE; **b** FTIR spectra of PME/GR-CPE; **c** SEM image of GR-CPE; **d** SEM image of PME/GR-CPE



process. The linear part corresponds to the diffusion-limiting electrochemical process. Figure 3b displayed the nyquist plots of different electrodes in 0.1 M KCl solution containing 5 mM  $[\text{Fe}(\text{CN})_6]^{3-/4-}$  probe. A large  $R_{\text{ct}}$  with a value of about 38.0  $\text{k}\Omega$  was obtained (curve a), indicating an inefficient electron-transfer process of redox probes at the surface of CPE. The  $R_{\text{ct}}$  value decreased to 18.3  $\text{k}\Omega$  after doping of graphene (curve b), which was mainly attributed to the high conductivity of graphene. A much lower  $R_{\text{ct}}$  (6.4  $\text{k}\Omega$ ) at the PME/GR-CPE surface was obtained, indicating the PME accelerated the electron communication between the redox couple  $[\text{Fe}(\text{CN})_6]^{3-/4-}$  and the electrode surface. The fast electron-transfer kinetics demonstrated the potential of modified CPE for sensing applications.

### Electrochemical behavior of BPA and HQ

The cyclic voltammetric behaviors of BPA and HQ on different electrodes were investigated. Figure 4 showed the CV curves of  $3.0 \times 10^{-4}$  M BPA and  $3.0 \times 10^{-4}$  M HQ in 0.1 M phosphate buffer (pH 7.0). The current responses of both BPA and HQ were improved on GR-CPE compared with that on bare CPE. The improvement indicated that graphene promotes electron transport and communication between the solution and electrode due to the excellent conductivity. This result also confirmed the good electrocatalytic activity of graphene towards to BPA and HQ. On the PME/GR-CPE, the peak currents of BPA and HQ significantly increased compared with those on the bare CPE and GR-CPE, which was

**Fig. 3** (a) CVs of a CPE, b GR-CPE, c PME/GR-CPE in 0.1 M KCl solution containing 5.0 mM  $\text{K}_3\text{Fe}(\text{CN})_6$ . (b) Nyquist plots of a CPE, b GR-CPE, c PME/GR-CPE in 0.1 M KCl solution containing 5.0 mM  $[\text{Fe}(\text{CN})_6]^{3-/4-}$

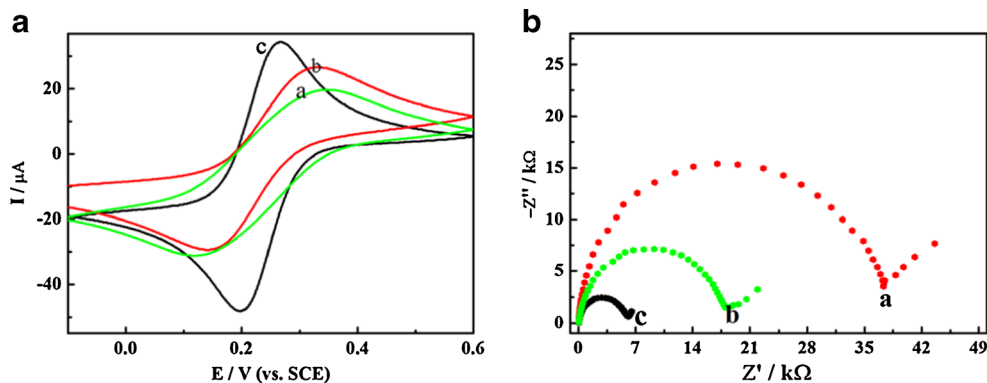
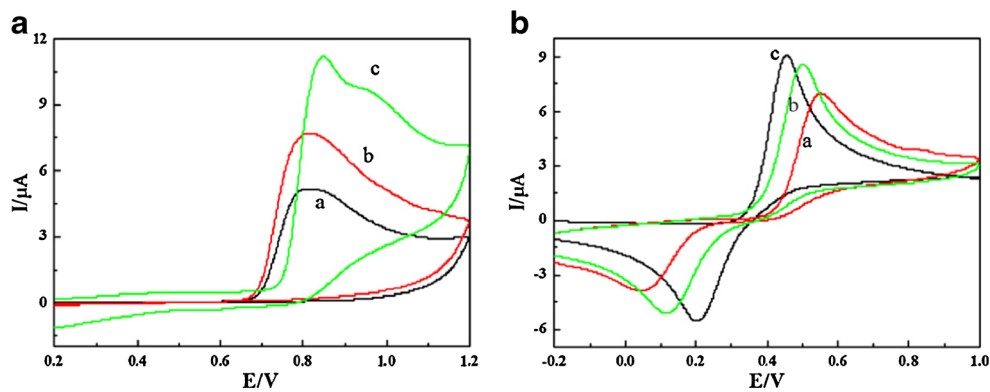


**Fig. 4** Cyclic voltammograms of **a**  $3.0 \times 10^{-4}$  M BPA; **b**  $3.0 \times 10^{-4}$  M HQ on different electrodes: (a) CPE; (b) GR-CPE; (c) PME/GR-CPE



attributed the high surface area and adsorptive capacity of PME/GR-CPE. The nitrogen-rich and aromatic features of PME are believed to interact with BPA or HQ through hydrogen bonding and  $\pi$ - $\pi$  interactions, respectively. The combination of the both effects is suggested to be responsible for the enhanced current responses.

The CVs of the mixture of  $3.0 \times 10^{-4}$  M BPA and  $3.0 \times 10^{-4}$  M HQ at different electrodes were shown in Fig. 5. The oxidation peak of HQ overlapped with that of BPA at CPE (curve a) and GR-CPE (curve b). However, the two well-defined peaks at 0.35 and 0.65 V were clearly shown on PME/GR-CPE, corresponded to the oxidation of HQ and BPA, respectively. These peaks were well separated and showed a potential difference of about 300 mV, which was an adequately large window for simultaneous detection of BPA and HQ in the mixed solutions. The oxidation currents of both HQ and BPA on the PME/GR-CPE are higher compared to a plain CPE and a GR-modified CPE. The high current responses were beneficial for the following sensing applications.

### Optimization of method

The effects of pH and scan rates on the peak currents were investigated. Respective data and figures are given in the

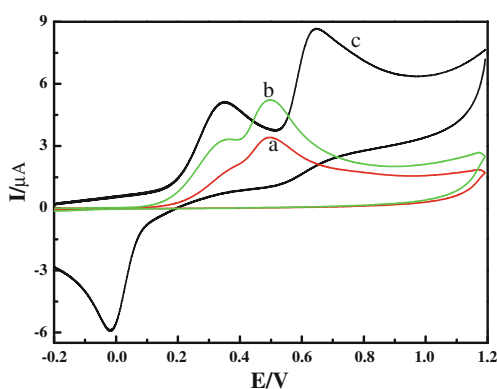


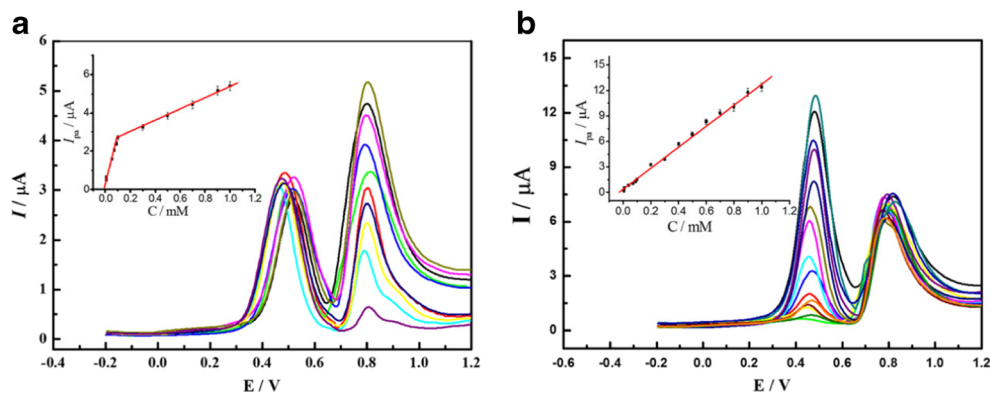
**Fig. 5** Cyclic voltammograms of mixture of  $3.0 \times 10^{-4}$  M HQ and  $3.0 \times 10^{-4}$  M BPA at **a** CPE, **b** GR-CPE, **c** PME/GR-CPE

Electronic Supporting Material (Fig. S1). The electrolyte with pH 2.5, scan rate of  $50 \text{ mV s}^{-1}$  were chosen for the following experiment. The oxidation peak currents of BPA and HQ were linear with the square root of scan rate ( $\nu^{1/2}$ ) in the range of 100–700  $\text{mV}\cdot\text{s}^{-1}$ . The regression equations were  $I_{\text{pa}} (\mu\text{A}) = -2.809 + 1.233 \nu^{1/2}$  ( $\text{mV}^{1/2}\cdot\text{s}^{-1/2}$ ) ( $R = 0.997$ ) for BPA,  $I_{\text{pa}} (\mu\text{A}) = 0.168 + 0.970 \nu^{1/2}$  ( $\text{mV}^{1/2}\cdot\text{s}^{-1/2}$ ) ( $R = 0.992$ ) for HQ, respectively, indicating that the electrode reactions of HQ and BPA at PME/GR-CPE are diffusion-controlled processes [18].

### Simultaneous determination of HQ and BPA using DPV

For simultaneous determination of BPA and HQ using PME/GR-CPE sensor, differential pulse voltammetry (DPV) was carried out under the optimized conditions. Figure 6a showed the DPV curves for different concentrations of BPA coexisting with HQ. The peak currents of BPA increased with increasing the concentration with two linear parts. The linear equations (inset of Fig. 6a) were  $I_{\text{pa}} (\mu\text{A}) = 0.371 + 23.269 C$  (mM) ( $R = 0.998$ ) in the range of  $9.0 \times 10^{-6} \sim 1.0 \times 10^{-4}$  M and  $I_{\text{pa}} (\mu\text{A}) = 2.355 + 3.062 C$  (mM) ( $R = 0.999$ ) in the range of  $1.0 \times 10^{-4} \text{ M} \sim 1.0 \times 10^{-3} \text{ M}$  with a detection limit of  $1.05 \times 10^{-8}$  M, respectively. As shown in Fig. 6b, the peak currents of HQ enhanced linearly with increasing the concentration of HQ. The linear equation (inset of Fig. 6b) was  $I_{\text{pa}} (\mu\text{A}) = 0.343 + 12.541 C$  (mM) ( $R = 0.998$ ) in the range of  $7.0 \times 10^{-6} \text{ M} \sim 1.0 \times 10^{-3} \text{ M}$  with a detection limit of  $7.4 \times 10^{-8}$  M. It was found that the presence of another substrate had no effect on the peak currents and potentials on the target analyte. Compared with other HQ or BPA electrochemical sensors with DPV techniques listed in Table 1, the sensor exhibited a lower detection limit and wider linear range. This result can be attributed to the synergistic effect between the graphene and PME. The remarkable conductivity, electrocatalytic activity of graphene and the adsorptive capability of PME may be the main contribution that can amplify the current signals and lowered the detection limit. Therefore, the PME/GR-CPE

**Fig. 6** **a** DPV curves of various concentrations of BPA in the presence of  $3.0 \times 10^{-4}$  M HQ, Inset is the relationship between concentrations of BPA and peak currents. **b** DPV curves of various concentrations of HQ in the presence of  $3.0 \times 10^{-4}$  M BPA, Inset is the relationship between concentrations of HQ and peak currents



sensor is a competitive candidate for simultaneous detection of HQ and BPA.

### Reproducibility, stability and interference study

To evaluate the fabrication reproducibility of the sensor, the oxidation peak currents of  $3.0 \times 10^{-4}$  M HQ and  $3.0 \times 10^{-4}$  M BPA on six PME/GR-CPE sensors with same fabrication procedures were measured. All of the sensors exhibited similar current responses with a relative standard deviation (RSD) of 2.8% and 3.5% for HQ and BPA, respectively. When the sensor was not in use, it was stored in a refrigerator at 4 °C.

Initial responses of over 95.6% and 88.4% were maintained after storage for 15 and 30 days, respectively, indicating the good stability of the sensor.

In order to evaluate the selectivity of the sensor, the influences of various possible interferences on the determination of  $3.0 \times 10^{-4}$  M HQ and  $3.0 \times 10^{-4}$  M BPA was investigated by DPV, as shown in Fig. 7. It was found that 10 mM  $Zn(NO_3)_2$ , KCl,  $MgCl_2$ ,  $CaCl_2$ ,  $Na_2SO_4$ , catechol, 2-nitrophenol, 3-nitrophenol, 4-nitrophenol, aniline, humic acid and hydroxyflavonoids did not interfere with the determination of HQ and BPA in the present system (signal change below 5%). However, 10 mM resorcinol and paracetamol coexisting

**Table 1** Comparison of different modified electrodes for detection of BPA and HQ with DPV techniques

| Sample | Electrode                | Working potential | Liner range( $\mu$ M) | Detection limit ( $\mu$ M) | Refs      |
|--------|--------------------------|-------------------|-----------------------|----------------------------|-----------|
| BPA    | gold nanodendrites/GCE   | 0.2–0.7           | 0.05–55.0             | 0.0012                     | [16]      |
|        | $SiO_2/GO/AgNP$          | 0.3–0.9           | 0.1–2.6               | 0.127                      | [41]      |
|        | $MoS_2/SPAN/GCE$         | 0.1–0.9           | 0.001 ~ 1.0           | 0.0006                     | [19]      |
|        | $\beta$ -CD/IL-CPE       | 0.2–1.0           | 0.1 ~ 11              | 0.083                      | [42]      |
|        | $PGA/MWCNT-NH_2/GCE$     | 0.2–1.8           | 0.1 ~ 10              | 0.02                       | [17]      |
|        | $Bi_2WO_6$ -CPE          | 0–0.8             | 0.07 ~ 1.3            | 0.02                       | [18]      |
|        | Pt/Graphene-CNTs         | 0–1.0             | 0.06 ~ 10<br>10 ~ 80  | 0.042                      | [20]      |
|        | PME/GR-CPE               | –0.2–1.2          | 9 ~ 100<br>100 ~ 1000 | 0.0105                     | This work |
| HQ     | $SiO_2/C$ electrode      | –0.2–0.6          | 39 ~ 1250             | 1.6                        | [43]      |
|        | BG/GCE                   | –1–4              | 5.0 ~ 100             | 0.3                        | [44]      |
|        | CNCs-RGO/GCE             | –0.2–0.8          | 1.0 ~ 400             | 0.87                       | [21]      |
|        | PEDOT/NGE/GCE            | –0.2–0.6          | 1.0 ~ 10              | 0.18                       | [45]      |
|        | $GR/MWCNTs/BMIMPF_6/GCE$ | –0.1–0.5          | 0.5 ~ 2900            | 0.1                        | [46]      |
|        | $WS_2$ -GR/GCE           | –0.2–0.8          | 1.0 ~ 100             | 0.1                        | [22]      |
|        | PME/GR-CPE               | –0.2–1.2          | 7.0 ~ 1000            | 0.074                      | This work |

$MoS_2/SPAN/GCE$ : molybdenum disulfide/self-doped polyaniline modified glassy carbon electrode.

$\beta$ -CD/IL CPE:  $\beta$ -cyclodextrin ( $\beta$ -CD) modified ionic liquid based carbon paste electrode.

$PGA/MWCNT-NH_2/GCE$ : polyglutamate acid (PGA) and amino-functionalised carbon nanotubenanocomposite modified glassy carbon electrodes.

BG/GCE: boron-doped graphene (BG) modified glass carbon electrode (GCE).

CNCs-RGO/GCE: carbon nanocages (CNCs)-reduced graphene oxide (RGO) modified glass carbon electrode.

PEDOT/NGE/GCE: poly(3,4-ethylenedioxythiophene) /nitrogen-doped graphene composites modified glassy carbon electrode (GCE).

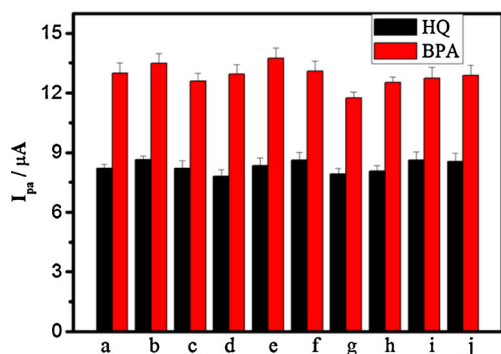


**Fig. 7** The currents of  $3.0 \times 10^{-4}$  MHQ and  $3.0 \times 10^{-4}$  M BPA in the absence **a** and presence of 10 mM various interferences (from **b** to **j**):  $\text{Zn}^{2+}$ ,  $\text{Na}^+$ ,  $\text{Ca}^{2+}$ ,  $\text{Mg}^{2+}$ ,  $\text{K}^+$ , 2-nitrophenol, 3-nitrophenol, 4-nitrophenol, catechol

with  $3.0 \times 10^{-4}$  M HQ and  $3.0 \times 10^{-4}$  M BPA have some effects on the current response due to the similar oxidation peak potential. While the concentration of resorcinol and paracetamol below 1.0 mM, it did not interfere with the determination of HQ and BPA. The selectivity of this sensor was attributed to the adsorption and accumulation of BPA and HQ due to the interaction between amine groups of PME and the phenolic groups of BPA and HQ.

### Real sample analysis

To evaluate the practical application of the PME/GR-CPE sensor for real sample analysis, the concentration of BPA and HQ in tap water and wastewater samples was determined with the standard addition method. Results showed recoveries ranging from 97.25% to 103.5% and RSDs ranging from 0.10% to 2.10% (Table 2), indicating the practical applicability and reliability of the sensor.

### Conclusions

A sensor based on PME/GR-CPE was fabricated through a facile doping and electro-polymerization method. Utilizing

**Table 2** Determination of HQ and BPA in tap-water and wastewater samples ( $n = 3$ )

| Sample     | Added(μM) |      | Founded(μM) |      | RSD (%) |      | Recovery (%) |       |
|------------|-----------|------|-------------|------|---------|------|--------------|-------|
|            | BPA       | HQ   | BPA         | HQ   | BPA     | HQ   | BPA          | HQ    |
| Tap -water | 40.0      | 60.0 | 40.8        | 59.5 | 1.17    | 0.42 | 102.1        | 99.14 |
|            | 70.0      | 80.0 | 68.7        | 82.1 | 0.87    | 1.02 | 98.19        | 102.7 |
|            | 20.0      | 30.0 | 20.3        | 29.9 | 0.92    | 2.10 | 101.7        | 99.68 |
| Wastewater | 40.0      | 60.0 | 38.9        | 62.1 | 1.21    | 0.72 | 97.25        | 103.5 |
|            | 70.0      | 80.0 | 68.6        | 79.5 | 0.85    | 1.19 | 97.94        | 99.37 |
|            | 20.0      | 30.0 | 19.9        | 29.3 | 0.89    | 0.10 | 99.50        | 97.68 |

the excellent conductivity and electrocatalytic activity of graphene, the adsorptive capability of PME, the sensor exhibited superior performance such as high sensitivity and stability to the simultaneous detection of HQ and BPA. The sensor was applied in detection of HQ and BPA in tap water and wastewater samples. Furthermore, PME based sensor can be implemented as a promising method for detection of phenol compounds in food and environment.

**Acknowledgment** We greatly appreciate the support of University Science and Technology Research Project of Ningxia Province (NGY2015050) and the National Natural Science Foundation of China (No: 21265014). This work is also supported by State Key Laboratory of Analytical Chemistry for Life Science (SKLACLS1421) and Enhance Comprehensive Strength Project of Ningxia University (8016-18).

**Compliance with ethical standards** The author(s) declare that they have no competing interests.

### References

- Schechter A, Malik N, Haffner D, Smith S, Harris TR, Paepke O, Birnbaum L (2010) Bisphenol a (BPA) in U.S. food. *Environ Sci Technol* 44:9425–9430
- Beausoleil C (2015) Practical example of a WoE-approach with BPA and other endocrine disruptor compounds. *Toxicol Lett* 238:S32–S55
- Deblonde T, Cossu C, Hartemann P (2011) Emerging pollutants in waste water: a review of the literature. *Int J Hyg Environ Health* 214:442–448
- Lorber M, Schechter A, Paepke O, Shropshire W, Christensen K, Birnbaum L (2015) Exposure assessment of adult intake of bisphenol a (BPA) with emphasis on canned food dietary exposures. *Environ Int* 77:55–62
- Salian S, Doshi T, Vanage G (2011) Perinatal exposure of rats to bisphenol a affects fertility of male offspring-an overview. *Reprod Toxicol* 31:359–362
- Aom Saal FS, Vandevoor CA, Taylor JA, Welshons WV, Toutain PL, Hunt PA (2014) Bisphenol a (BPA) pharmacokinetics with daily oral bolus or continuous exposure via silastic capsules in pregnant rhesus monkeys: relevance for human exposures. *Reprod Toxicol* 45:105–116
- Huang YQ, WCKC, Zheng JS, Bouwman BR, Wahlstrom B, Neretin L, Wong MH (2012) Bisphenol a (BPA) in China: a review of sources, environmental levels, and potential human health impacts. *Environ Int* 42:91–99
- Siew EL, Chan KM, Williams GT, Ross D, Inayat-Hussain SH (2012) Protection of hydroquinone-induced apoptosis by down regulation of Fau is mediated by NQO1. *Free Radic Biol Med* 53:1616–1624
- Chen LX, Kupferle MJ (2014) Development, validation and application of an HPLC method for phenol electrooxidation products in the presence of chloride. *Intern J Environ Anal Chem* 94:679–669
- Huan T, Wu Y, Tang C, Lin G, Li L (2015) Dn ID in my compound ID for rapid identification of dansylated amine- and phenol-containing metabolites in LC – MS-based metabolomics. *Anal Chem* 87:9838–9845
- Becena V, Odermatt J (2012) Detection and quantification of traces of bisphenol a and bisphenol S in paper samples using analytical pyrolysis-GC/MS. *Analyst* 137:2050–2059
- Xu SH, Li JL, Li XM, Su M, Shi ZM, Zeng Y, Ni SJ (2016) A chemiluminescence resonance energy transfer system composed of cobalt(II), luminol, hydrogen peroxide and CdTe quantum dots for

- highly sensitive determination of hydroquinone. *Microchim Acta* 183:667–673
13. Deng C, Zhong YP, He Y, Ge YL, Song GW (2016) Selective determination of trace bisphenol a using molecularly imprinted silica nanoparticles containing quenchable fluorescent silver nanoclusters. *Microchim Acta* 183:431–439
  14. Zou YS, Lou D, Dou K, He LL, Dong YH, Wang SL (2016) Amperometric tyrosinase biosensor based on boron-doped nanocrystalline diamond film electrode for the detection of phenolic compounds. *J Solid State Electr* 20:47–54
  15. Yin HS, Zhou YL, Ai SY, Han RX, Tang TT, Zhu LS (2010) Electrochemical behavior of bisphenol a at glassy carbon electrode modified with gold nanoparticles, silk fibroin, and PAMAM dendrimers. *Microchim Acta* 170:99–105
  16. Chen WY, Mei LP, Feng JJ, Yuan T, Wang AJ, Yu H (2015) Electrochemical determination of bisphenol a with a glassy carbon electrode modified with gold nanodendrites. *Microchim Acta* 182:703–709
  17. Lin YQ, Liu KY, Liu CY, Yin L, Kang Q, Li LB, Li B (2014) Electrochemical sensing of bisphenol a based on polyglutamic acid/amino-functionalized carbon nanotubes nanocomposite. *Electrochim Acta* 133:492–500
  18. Peng L, Dong SY, Xie HD, Gu GZ, He ZX, Lu JS, Huang TL (2014) Sensitive simultaneous determination of diethylstilbestrol and bisphenol a based on Bi<sub>2</sub>WO<sub>6</sub> nanoplates modified carbon paste electrode. *J Electroanal Chem* 726:15–20
  19. Yang T, Chen H, Yang R, Jiang Y, Li W, Jiao K (2015) A glassy carbon electrode modified with a nanocomposite consisting of molybdenum disulfide intercalated into self-doped polyaniline for the detection of bisphenol a. *Microchim Acta* 182:2623–2628
  20. Zheng ZX, Du YL, Wang ZH, Feng QL, Wang CM (2013) Pt/graphene–CNTs nanocomposite based electrochemical sensors for the determination of endocrine disruptor bisphenol a in thermal printing papers. *Analyst* 138:693–701
  21. Huang YH, Chen JH, Sun X, Su ZB, Xing HT, Hu SR, Weng W, Guo HX, Wu WB, He YS (2015) One-pot hydrothermal synthesis carbon nanocages-reduced graphene oxide composites for simultaneous electrochemical detection of catechol and hydroquinone. *Sensors Actuators B Chem* 212:165–173
  22. Huang KJ, Wang L, Liu YJ, Gan T, Liu YM, Wang LL, Fan Y (2013) Synthesis and electrochemical performances of layered tungsten sulfide-graphene nanocomposite as a sensing platform for catechol, resorcinol and hydroquinone. *Electrochim Acta* 107:379–387
  23. Yang L, Zhao H, Fan SM, Li BC, Li CP (2014) A highly sensitive electrochemical sensor for simultaneous determination of hydroquinone and bisphenol a based on the ultrafine Pd nanoparticle@TiO<sub>2</sub> functionalized SiC. *Anal Chim Acta* 852:28–36
  24. Pincak R, Smotlacha J (2013) Analogies in electronic properties of graphene wormhole and perturbed nanocylinder. *Eur Phys J B* 86:480–486
  25. Liu H, Li YH, Dai K, Zheng GQ, Liu CT, Shen CY, Yan XR, Guo J, Guo ZH (2016) Electrically conductive thermoplastic elastomer nanocomposites at ultralow graphene loading levels for strain sensor applications. *J Mater Chem C* 4:157–166
  26. Shen RY, Zhang WM, Yuan Y, He GY, Chen HQ (2015) Electrochemical detection of bisphenol a at graphene/melamine nanoparticle-modified glassy carbon electrode. *J Appl Electrochem* 45:343–352
  27. Ntsendwana B, Mamba BB, Sampath S, Arotiba OA (2012) Electrochemical detection of bisphenol a using graphene-modified glassy carbon electrode. *Int J Electrochem Sci* 7:3501–3512
  28. Lei W, Si W, Xu Y, Gu Z, Hao Q (2014) Conducting polymer composites with graphene for use in chemical sensors and biosensors. *Microchim Acta* 181:707–722
  29. Ghanbari K, Hajheidari N (2015) ZnO–Cu<sub>x</sub>O/polypyrrole nanocomposite modified electrode for simultaneous determination of ascorbic acid, dopamine, and uric acid. *Anal Biochem* 473:53–62
  30. Fang Y, Jiang Q, Deng M, Tian Y, Wen Q, Wang MF (2015) Preparation in-situ of carbon nanotubes/polyaniline modified electrode and application for ascorbic acid detection. *J Electroanal Chem* 755:39–46
  31. Gu HB, Guo J, Wei HG, Yan XR, Ding DW, Zhang X, He QL, Sruthi T, Wang XF, Thomas H, Wei SY, Guo ZH (2015) Transparent anhydride-cured epoxy nanocomposites reinforced with polyaniline stabilized nanosilica. *J Mater Chem C* 3:8152–8165
  32. Zhou XF, Song YH, He KY, Zheng HT, Suye SI (2015) Electrochemical preparation and application of PEDOT/ferrocene modified electrode. *Applied Mechanics and Materials* 727–728:61–64
  33. Ruan CQ, Shi W, Jiang HR, Sun YN, Liu X, Zhang XY, Sun Z, Dai LF, Ge DT (2013) One-pot preparation of glucose biosensor based on polydopamine–graphene composite film modified enzyme electrode. *Sensor Actuators B Chem* 177:826–832
  34. Zhang X, Yan XG, He QG, Wei HG, Long J, Guo J, Gu HB, Yu JF, Liu JJ, Ding DW, Sun LY, Wei SY, Guo ZH (2015) Electrically conductive polypropylene nanocomposites with negative permittivity at low carbon nanotube loading levels. *ACS Applied Materials Interfaces* 7:6125–6138
  35. Liu X, Luo L, Qing Y, Wu Q, Wei Y, Ye D (2012) A highly sensitive method for determination of guanine, adenine and epinephrine using poly-melamine film modified glassy carbon electrode. *J Electroanal Chem* 675:47–53
  36. Gupta P, Goyal RN (2014) Polymelamine modified edge plane pyrolytic graphite sensor for the electrochemical assay of serotonin. *Talanta* 120:17–22
  37. Su YL, Cheng SH (2015) Sensitive and selective determination of gallic acid in green tea samples based on an electrochemical platform of poly(melamine) film. *Anal Chim Acta* 901:41–50
  38. William SHJ, Richard EO (1958) Preparation of graphitic oxide. *J Am Chem Soc* 80:1339
  39. Liu P, Gong K (1999) Preparation and characterization of poly(vinyl acetate)-intercalated graphite oxide. *Carbon* 37:2073–2075
  40. Seo DH, Rider AE, Han ZJ, Kumar S, Ostrikov KK (2013) Plasma break-down and rebuild: same functional vertical graphenes from diverse natural precursors. *Adv Mater* 25:5638–5642
  41. Campos AM, Raymundo-Pereira PA, Cincotto FH, Canevari TC, Machado Sergio AS (2015) Sensitive determination of endocrine disruptor bisphenol a at ultrathin film based on nanostructured hybrid material SiO<sub>2</sub>/GO/AgNP. *J Solid State Electrochem* 17:1–5
  42. Yu XW, Chen YK, Chang LP, Zhou L, Tang FX, Wu XP (2013) β-cyclodextrin non-covalently modified ionic liquid-based carbon paste electrode as a novel voltammetric sensor for specific detection of bisphenol a. *Sensors Actuators B Chem* 186:648–656
  43. Canevari TC, Arenas LT, Landers R, Roxgério C, Gushikema Y (2013) Simultaneous electroanalytical determination of hydroquinone and catechol in the presence of resorcinol at an SiO<sub>2</sub>/C electrode spin-coated with a thin film of Nb<sub>2</sub>O<sub>5</sub>. *Analyst* 138:315–324
  44. Zhang YZ, Sun RX, Luo BM, Wang LJ (2015) Boron-doped graphene as high-performance electrocatalyst for the simultaneously electrochemical determination of hydroquinone and catechol. *Electrochim Acta* 156:228–234
  45. Si WM, Lei W, Han Z, Hao QL, Zhang YH, Xia MZ (2014) Selective sensing of catechol and hydroquinone based on poly(3,4-ethylenedioxythiophene)/nitrogen-doped graphene composites. *Sensors Actuators B Chem* 199:154–160
  46. Wang X, Wu M, Li H, Wang QJ, He PG, Fang YZ (2014) Simultaneous electrochemical determination of hydroquinone and catechol based on three-dimensional graphene/MWCNTs/BMIMPF<sub>6</sub> nanocomposite modified electrode. *Sensors Actuators B Chem* 192:452–458